Journal of Hydrology 624 (2023) 129894

Contents lists available at ScienceDirect

Journal of Hydrology

journal homepage: www.elsevier.com/locate/jhydrol

Research papers

Effects of glacier retreat upon glacier-groundwater coupling and biogeochemistry in Central Svalbard

Andrew Hodson[a,b,*], Gabrielle Kleber[a,c], Jack Johnson[d], Michael Lonardi[e], Chiara Petroselli[f], Tim Dixon[g], Simon Bottrell[g]

[a] Department of Arctic Geology, University Centre In Svalbard (UNIS), 9171 Longyearbyen, Norway
[b] Department of Environmental Sciences, Western Norway University of Applied Sciences, Sogndal, 5020 Bergen, Norway
[c] Department of Earth Sciences, University of Cambridge, CB2 3EQ, UK
[d] Department of Geography, University of Sheffield, Sheffield S10 2TN, UK
[e] Institute for Meteorology, University of Leipzig, 04103 Leipzig, Germany
[f] Department of Chemistry, Biology and Biotechnology, University of Perugia, 8 – 06123 Perugia, Italy
[g] School of Earth and Environment, University of Leeds, Leeds, LS2 8JT, UK

ARTICLE INFO

This manuscript was handled by Huaming Guo, Editor-in-Chief, with the assistance of Rafael Perez Lopez, Associate Editor

Keywords:
Intra-permafrost groundwater
Glacier – groundwater interaction
Arctic groundwater biogeochemistry
Sulfate reduction

ABSTRACT

The hydrology and biogeochemistry of perennial groundwater springs emerging in the forefields of retreating Svalbard glaciers are considered through a single-site, multi-year study at Foxfonna, and a multi-site spatial sampling programme during consecutive winter seasons. We show that such springs are commonplace in the forefields of retreating Svalbard glaciers, including even cold-based glaciers underlain by permafrost. The groundwaters all contain geogenic methane and are generally anoxic, but reveal a range of different redox environments linked to sulfide oxidation, denitrification and sulfate reduction. The principal source waters for these springs seems to be snow and firn meltwaters entering bergschrund crevasses at high elevation glacier margins. At Foxfonna, the glacier's strongly negative mass balance and transition to cold-based thermal conditions have resulted in reduced groundwater discharge into the proglacial river due to lower rates of recharge (less dilution). Throughout these changes, sulfide oxidation coupled to Na-Silicate weathering has remained a dominant reaction, driving a three-fold increase in electrical conductivity since 2010. The period has also been characterised by the complete loss of NO_3^- since summer 2018, as well as short-lived changes in the Oxidation-Reduction Potential and methane concentration. Therefore, climate-driven glacial retreat influences both the quantity and quality of groundwaters entering downstream drainage systems, which exist in spite of cold-based glaciers and permafrost being prevalent in this part of the Arctic.

1. Introduction

The hydrologic response of high Arctic glacier-fed rivers to climate change is greatly complicated by permafrost and the complex (poly) thermal structure of valley glaciers. Despite the known diversity of glacier thermal regimes in Svalbard (e.g. Sevestre et al., 2015) and its established sensitivity to climate-related processes (Van Pelt et al., 2016), we are poorly equipped to understand how changes in glacier thermal regime influence the hydrological cycle. Major complicating factors include the presence of permafrost (Etzelmüller and Hagen, 2005) and the transition that glaciers undergo from being polythermal to cold-based as they lose mass (e.g. Hodgkins et al., 1999). The latter has profound effects upon a range of hydrological and biogeochemical processes operating at the glacier bed (e.g. Hodson and Ferguson, 1999; Irvine-Fynn and Hodson, 2010; Nowak and Hodson, 2014). It is also likely to greatly affect groundwater recharge, movement and its downstream mixing with proglacial runoff. However, our understanding of the latter is greatly limited by a lack of observations that describe groundwater in permafrost environments (e.g. Chesnokova et al., 2020; Haldorsen et al., 2010), which means glacier – groundwater interaction in the polar regions is far less understood than elsewhere from both hydrological (e.g. Ó Dochartaigh et al., 2019; Vincent et al., 2019) and biogeochemical (e.g. Kristiansen et al., 2013) perspectives. These processes therefore deserve far greater research attention in the Arctic if we are to better understand watershed

---

* Corresponding author at: Department of Arctic Geology, University Centre In Svalbard (UNIS), 9171 Longyearbyen, Norway.
E-mail address: AndrewH@unis.no (A. Hodson).

https://doi.org/10.1016/j.jhydrol.2023.129894
Received 11 March 2023; Received in revised form 13 June 2023; Accepted 28 June 2023

hydrological functioning and the dynamics of nutrients, sediment and climate-relevant greenhouse gases such as methane (Kleber et al., 2023). As a consequence, there have now been several important studies of shallow groundwater dynamics in Svalbard glacier forefields (e.g. Cooper et al., 2002; Stachniak et al., 2022). However, major new insights into intra- and sub-permafrost groundwater coupling with glaciers (Nowak et al., 2020; Haldorsen et al., 2010; Szynkiewicz et al., 2020) or ice sheets (Scheidegger and Bense, 2014) are still urgently required as glaciers undergo rapid changes.

Nowak and Hodson (2014) demonstrated marked seasonal and annual changes in runoff biogeochemistry at Austre Broggerbreen following its transition to a cold-based glacier: a major perturbation brought about by glacier retreat and thinning. However, the system had already lost both its subglacial outflow at the glacier margin and a pressurised groundwater outflow some distance downstream, described during the 1940's by Orvin (1944). The same glacier has also been used in studies that employ space-for-time substitution to isolate the potential impact of subglacial drainage loss as a consequence of glacier thermal regime change: e.g. in the contexts of drainage system structure (Tranter et al., 1996) and nutrient export (Hodson et al., 2005). Wadham et al (2010) also compared glaciers, but instead isolated the effect of scale upon residence time and subglacial biogeochemistry to show how redox reactions not unlike those associated with long residence time sub-permafrost groundwaters (e.g. Lauritzen and Bottrell, 1994) typically only occur beneath the larger Arctic glaciers (see also Wadham et al., 2004). However, whilst these studies have emphasised the impact of glacier change upon glacial runoff biogeochemistry, none have directly addressed the biogeochemical implications of changing glacier-groundwater interaction.

Haldorsen et al (2010) showed how the recharge volumes of dilute glacial meltwater entering the sub-permafrost groundwater system can cease once a glacier has frozen to its bed by describing historical changes at Vestre Brøggerbreen in Svalbard. However, this work did not benefit from observations describing the system while the glacier still supported the groundwater system, and so few insights into the subglacial recharge processes were gained. By contrast, Smith et al (2002) observed geophysical evidence for subglacial recharge of sub-permafrost groundwater following the onset of a surge at Bakaninbreen, Central Svalbard. Frictional heating at the bed of the accelerating glacier was thought to thermally erode the permafrost, forming through-taliks that enabled groundwater recharge driven by the high water basal pressures associated with a surge. Such taliks are likely to form during climate-driven glacier advance as well (Etzelmüller and Hagen, 2005). They are also likely are likely to become important points for subglacial water (or groundwater) discharge once the glacier has retreated, as described by Wainstein et al (2014) in the Canadian Arctic and Kleber et al (2023) in Central Svalbard. The presence of artesian springs discharging into the forefields of many retreating Svalbard and Canadian glaciers testifies to their importance and since they typically carry meltwaters with the highest concentrations of labile nutrients, trace elements and major ions, their biogeochemical importance has not gone un-noticed (e.g. Wadham et al., 1998; Irvine-Fynn and Hodson, 2010; Skidmore and Sharp, 1999; Stachnik et al., 2016).

The purpose of this paper is to demonstrate that, contrary to expectation, groundwater outflows persist in the forefield of Arctic glaciers that have already transitioned from polythermal to cold-based, and thus have the capacity to influence catchment hydrological and biogeochemical functioning during rapid, climate-driven glacier retreat. We use a single site, Foxfonna, to describe changing glacier – groundwater interaction at a range of temporal scales during the summer, before considering the biogeochemistry of multiple groundwater springs discharging from neighbouring cold and polythermal-based glaciers using samples collected during the winter season. In so doing we aim to improve understanding of how glacier retreat in the Arctic influences groundwater dynamics from hydrological, biogeochemical and greenhouse gas perspectives.

2. Field site details

We present data from Foxfonna and other glaciers in the Breinosa area of Adventdalen, Svalbard (Fig. 1). Most glaciers lie upon the shales and sandstones of the Cretaceous and Paleocene, which all contain coals. Towards the eastern limit of the study area, older shales and mudstones crop out. These lie well below Foxfonna, because the strata are generally dipping (by ca. 3°) towards the south west. The unit beneath the most profitable coal seam in the area, the Firkanten Formation, is known for a significant pyrite content and a low carbonate content (Dixon, 2019). It is the Firkanten Formation that hosts the groundwater flowpath that we describe in detail at Foxfonna.

Permafrost thicknesses are up to ca. 450 m in the high mountains, yet down to ca. 100 m or less in the valley bottoms (Humlum et al., 2003). Marked climate warming has been revealed by permafrost borehole temperatures as deep as 80 m (Isaksen et al., 2007). A decline in glacier mass balance has also been obvious (Schuler et al., 2020), such that glaciers in the Breinosa area have lost between 50% and 80% of their volume since the 1900′s (Schytt Holmlund, 2020). At present, the only glaciers supporting temperate basal ice in the study region are Kokbreen, Drønbreen and Møysallbreen (see Fig. 1), according to unpublished ground penetrating radar surveys. In spite of this, groundwater springs currently discharge highly mineralised, sub-oxic or anoxic water all year from the forefields of almost all the glaciers present (see Fig. 1).

Above the highest elevation spring, found at Foxfonna, a commercial coal seam crops out which has been mined since the 1970′s. Meltwater from the upper part of Foxfonna is known to exploit a crevassed zone (Fig. 2) and cause periodic flooding in the mine. This water is pumped out of the system into another catchment to the west, which we exclude from the present study in order to focus upon natural drainage systems. However, the presence of the mine greatly improves our understanding of permafrost at Foxfonna, and so we give particular attention to this site. Rock wall temperatures in the coal seam clearly show that permafrost propagates beneath Foxfonna, although the temperatures are marginally higher where the glacier is thickest (Christiansen et al., 2005). Boreholes drilled to the bed of Foxfonna's ablation area in the 1970′s also showed temperatures in subglacial ice were below the pressure melting point (Liestøl, 1974). However, broad swathes of the glacier bed were most likely at the pressure melting point in the late 19th Century, when photographic evidence shows Foxfonna was significantly thicker (Schytt Holmlund, 2020). Evidence for the previous existence of warm, basal ice include the abundant striations in the glacier forefield.

The groundwater system at Foxfonna discharges under artesian pressure all year from a steep section of ice cored moraine at ca. 320 m, before mixing with meltwater from an englacial drainage network connected to a deeply incised channel that descends a palaeo-crevasse at ca. 450 m elevation (Fig. 2). The presence of permafrost beneath the glacier means that the system represents an intra-permafrost aquifer. Its discharge from buried ice distinguishes it from the other sites in Fig. 1, where groundwater springs discharge via the proglacial outwash plains, presumably due to the presence of taliks. The large volume of buried glacier ice preserved beneath the floodplain at Foxfonna is currently ablating, causing great changes to the landscape and the course of the drainage system after its emergence.

The Proglacial Spring discharge at Foxfonna demonstrates no visible change on a diurnal basis but seems to be declining in recent years. The small artesian outflow has been present at least since the 1960′s and has gradually migrated in a northerly direction by ca. 100 m since 2010. Like all the perennial springs in Fig. 1, there is no discernible suspended sediment content, suggesting minimal contact with subglacial till. This is surprising given the great volume of finely comminuted moraine material filling the valleys, but demonstrates the impact of having a subglacial thermal regime dominated by cold-based ice (Hodson and Ferguson, 1999). The Proglacial Spring is also discernible by the odor of H_2S and by a distinct ochre deposit that forms around the discharge

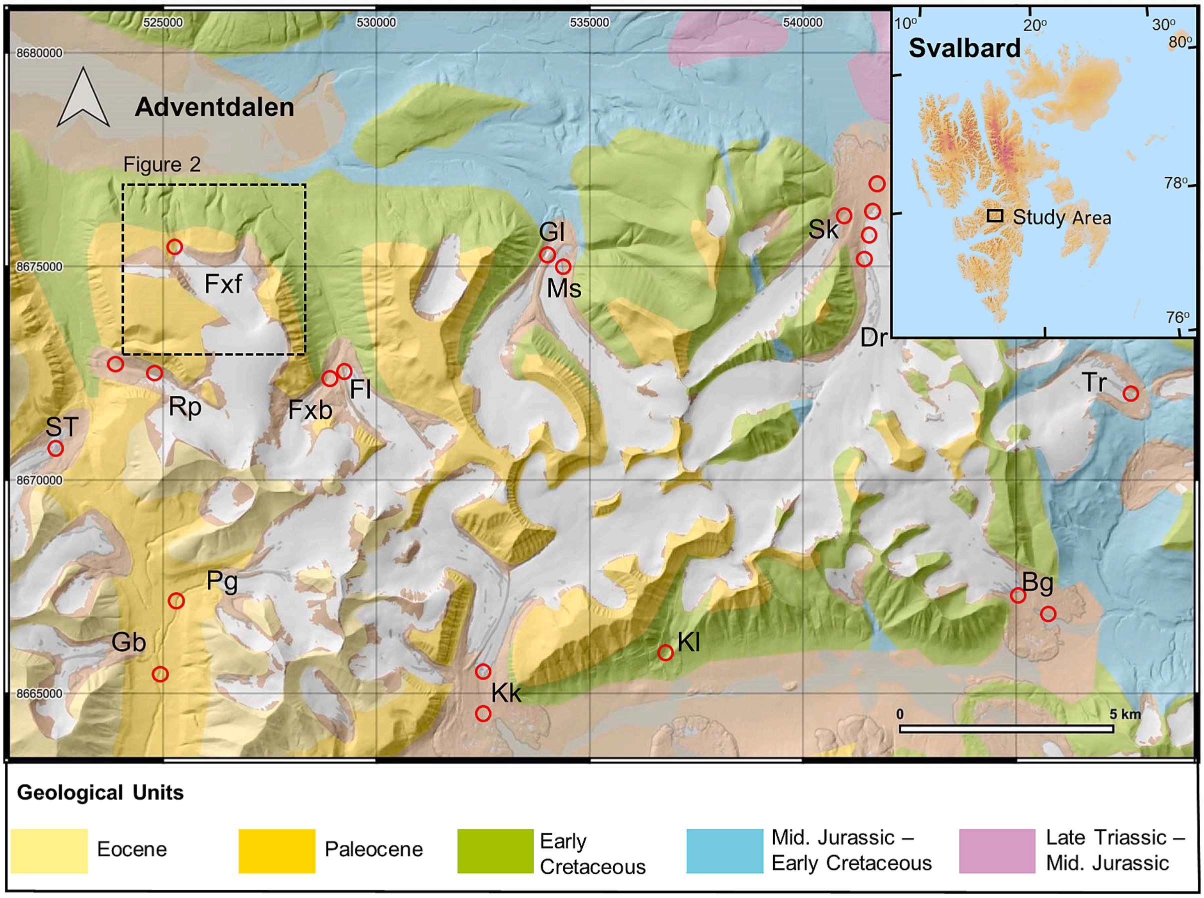

Fig. 1. Distribution of major geological units and glaciers in the Breinosa area. Foxfonna (Fx) (outlined by box) and other glaciers with perennial groundwater springs in their forefields are annotated. Red circles denote where such springs were found and sampled. Glacier names are: Foxfonna (Fxf), Rieperbreen (Rp), Scott Turnerbreen (ST), Gibsonbreen (Gb), Plogbreen (Pg), Kokbreen (Kk), Kilebreen (Kl), Bergmesterbreen (Bg), Tronisen (Tr), Drønbreen (Dr), Skoltbreen (Sk), Møysallbreen (Ms), Glottfjellbreen (Gl), Fleinisen (Fl) and Foxbreen (Fxb).

point. These features are also seen at other sites in Fig. 1 and demonstrate anoxic conditions in some, but not all, of the ground waters.

3. Methods

3.1. Hydrological monitoring

Continuous, hourly monitoring of bulk runoff and groundwater outflow in front of Foxfonna were undertaken in 2010, 2014, 2018 and 2019. In both 2010 and 2014, a bulk runoff station station was installed within 400 m of the glacier terminus (Upper Bulk Station), whilst in 2018 and 2019, the station was installed ca. 1 km downstream (Lower Bulk Station), which was necessitated by the disappearance of the proglacial stream into the moraines after the ablation of buried ice in the glacier forefield. Each year, we employed Campbell Scientific CR10x data loggers with Druck Pressure Transducers and CS-247 electrical conductivity and water temperature sensors. In 2018 and 2019, we also monitored CH_4 (details below) at the Proglacial Spring in the glacier forefield. Intermittent periods of electrical conductivity logging were also undertaken at the spring during 2010 (July), 2013 (August) and 2014 (July and August).

3.2. Geochemical sampling and analysis at Foxfonna during summer

We report detailed measurements of cation (Ca^{2+}, Mg^{2+}, Na^{+}, K^{+}) and anion (Cl^{-}, NO_3^{-}, SO_4^{2-}) concentrations in the Proglacial Spring throughout three summers (2014, 2018 and 2019). In addition, Fe, Mn, and CH_4 are reported for samples from 2018 and 2019. These groundwater samples are compared with samples from elsewhere in the watershed. For example, in 2014 it was possible to collect samples from the glacier river both prior to and after mixing with the Proglacial Spring (hereafter the "Eastern Portal" and "Upper Bulk Station", respectively: Fig. 2). In 2018 it was only possible to collect additional samples of bulk runoff from much further downstream ("Lower Bulk Station": Fig. 2). This was not repeated in 2019 because great changes in the composition of the water were observed as a consequence, and these changes seemed to result from shallow (seasonal) groundwater inputs and hyporheic processes not relevant to the groundwater system under study. We also compare data acquired from the comprehensive geochemical sampling described above to the results of more opportunistic sampling at the Proglacial Spring during 2010 and 2022. These were included to help confirm the longer-term changes revealed by the above sampling campaigns.

Each time a sample was collected, the pH, EC, dissolved O_2 and the oxidation–reduction potential (ORP) were recorded using Hach HQ40d meters and electrodes, calibrated using the manufacturer's calibration solutions. ORP is only reported from the Proglacial Spring because no significant oxygen demand was detected at any of the other sampling stations (rendering their ORP values unimportant). O_2 was either present at near-saturation (Eastern Portal or the two Bulk Sites) or absent in the anoxic Proglacial Spring, making the presentation of these data unnecessary as well. After these electrode measurements, syringe filtration of water samples through 0.45 μm cellulose nitrate filter papers was undertaken on site. Separate samples were collected for ions (50 mL) and Fe + Mn (15 mL) using pre-rinsed Corning centrifuge tubes. The 50 mL ion samples were filled without a headspace in the bottle and

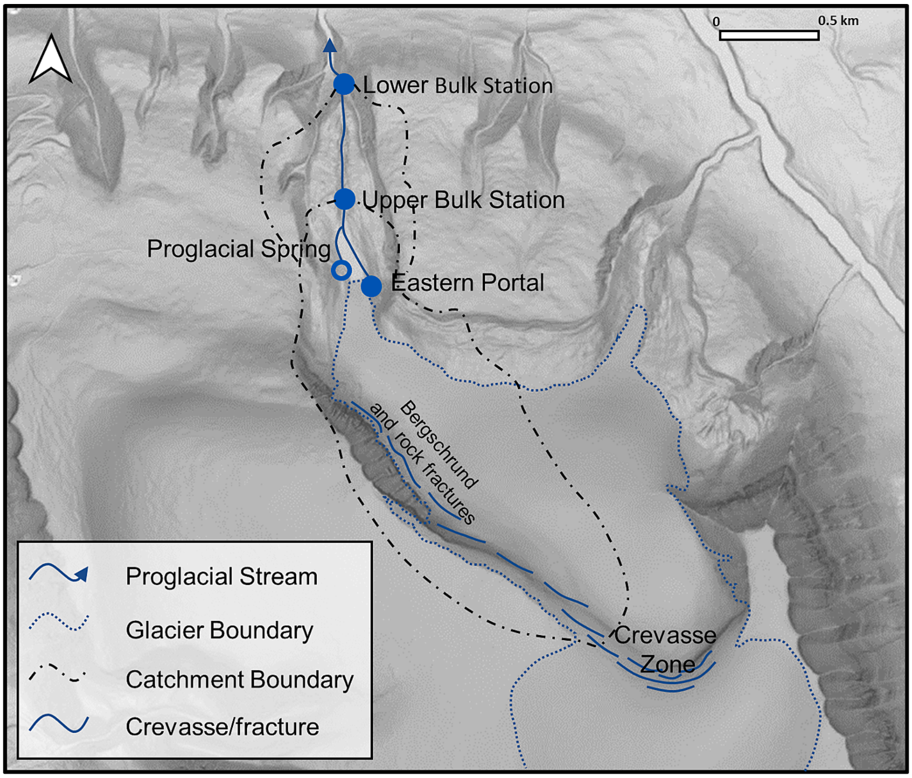

Fig. 2. Detail of the outlined area in Fig. 1, including Foxfonna, its catchment characteristics and the different sampling and monitoring sites used in the study.

analysed as soon as possible (within 2 months) after 4 °C storage in the dark. The 15 mL tubes were acidified to pH < 2 using 0.1 mL of concentrated HNO_3. Analytical techniques included Dionex ion chromatography (Dionex ICS-2100 chromatograph for simultaneous anion and cation detection in 2018, otherwise two Dionex ICS90 chromatographs for separate anion and cation determination), equipped with a Dionex IonPac AS15 and CS12A guard columns and IonPac AS15 and CS12 analytical columns. The detection limit was 0.06 mg L^{-1} or better for undiluted analyses and precision errors were < 5% according to repeat analyses of mid-range standards. Fe and Mn were analysed using Inductively Coupled Plasma Mass Spectrometry or ICP-MS (PerkinElmer Elan DRC II, MA, USA) with precision errors < 5% and a detection limit of 1.0 µg L^{-1}.

Methane was monitored on-site using a Pro-Oceanus MiniCH_4 detector, which works on the principle of headspace equilibration through a gas-permeable membrane that protects an infra-red detector from the water. The detection limit was 0.041 mg L^{-1}. Although factory-calibrated, we employed a field sample calibration in the range 0 – 41 mg L^{-1} using samples collected from a multitude of methane seeps in the area and analysed using gas-chromatography on a Shimadzu GC-2014 instrument equipped with a methaniser and flame ionisation detector. Full details are presented by Hodson et al (2020).

3.3. Geochemical sampling in winter

Fig. 1 reveals the sampling location of active groundwater springs that flow from the glacier forefields throughout the winter. Sampling followed the same procedure as described above, but was only conducted after locating the spring source beneath the icings created by groundwater refreezing. In many cases, these were easily discerned by the morphology of the icings and also the clear presence of water revealed by large ice blisters. A 5 cm Kovacs ice auger was then used to drill through the ice to enable abstraction of the water following minimal contact with the atmosphere. Sampling was conducted throughout late winter from 2019 to 2022. Further details are provided by Kleber et al (2023).

3.4. Stable isotopes

The stable carbon isotope composition ($\delta^{13}C$) of dissolved inorganic carbon (DIC) was determined for Foxfonna Proglacial Spring waters collected in summer 2019, and on all winter spring samples collected from the sites in Fig. 1. Samples were collected directly from the spring using a 22 mL Wheaton bottle with a crimp-top lid that was filled without a headspace. Samples were stored at 4 °C inverted and in the dark until analysis. Sample volumes of 1.5 mL were acidified with three or four drops of orthophosphoric acid (100%) in reaction vials flushed with helium gas. Samples were left to react for one hour before being transferred to a Thermo Gas Bench and CTC CombiPal Autosampler and the resulting CO_2 in the headspace was analysed using a Thermo Delta V Mass Spectrometer. Results are reported with reference to the international standard VPDB.

Stable isotopes of hydrogen and oxygen (δ^2H, $\delta^{18}O$) in water samples were analysed using a Picarro Cavity Ringdown Spectrometer. To minimize inter-sample memory effects, nine consecutive measurements were made of each sample. The first three measurements were discarded, and an average value was taken of the remaining six. Results are reported with reference to the international standard VSMOW.

Finally, stable isotope measurements of $\delta^{34}S$-SO4 were undertaken where there was sufficient SO_4^{2-} in the sample. Samples that had been syringe-filtered through 0.45 µm cellulose nitrate filters and acidified to pH < 2 with HNO_3 in the field were used for the measurement. Barium chloride ($BaCl_2$) solution was added to samples and left overnight to precipitate barite ($BaSO_4$), which was rinsed with MilliQ three times and then dried in a 70 °C oven. Approximately 400–500 µg of the dried precipitate was weighed into tin capsules and sealed along with an equal amount of vanadium pentoxide (V_2O_5) to aid in combustion. Samples were measured using a continuous flow GS-IRMS with a flash elemental analyzer (EA) and corrected to NBS 127 (20.3‰) and S06 (-34.2‰). Values are reported with reference to standard VCDT.

3.5. Flow separation of the seasonal hydrograph

A chemically-based mixing model was used to separate outflow from the Proglacial Spring (Qs) and glacial runoff (Qg, dominated by the Eastern Portal discharge) components from bulk discharge (Qb, at the Upper Bulk Station). The approach was made possible by the fact that concentrations of a suitable natural tracer for these components (i.e. Cs, Cg and Cb respectively) could be established by sampling immediately before and after they mixed during 2014. Sampling therefore lacked uncertainties linked to post-mixing reactions and inaccessibility that have affected the use of such models with subglacial hydrology (see Sharp et al., 1995). The mixing model took the form:

$$Q_bC_b = Q_gC_g + Q_sC_s \tag{1}$$

and since,

$$Q_b = Q_g + Q_s \tag{2}$$

then:

$$Qs = Qb(Cb\text{-}Cg)/(Cs\text{-}Cg) \tag{3}$$

Where Qs, Qg and Qb are the spring, glacial and bulk discharges in m^3/s and Cs, Cg and Cb are the concentrations of the chosen conservative tracer in mg L^{-1}. We found that Na^+ was ideal because it yielded one of the greatest concentration differences between Cs and Cg and it was readily detectable with low analytical precision error. Values of Na^+ from the spring, glacier river and bulk discharge sampling in 2014 were therefore used to estimate the component flows for this season only. During other years, including those when sampling was most frequent (2018 and 2019), flow separation could not be achieved because Qb could only be sampled ca. 1 km downstream and after multiple inputs of several Na^+-enriched shallow groundwater springs and moraine waters.

4. Results

4.1. Hydrology

Seasonal hydrographs describing the bulk runoff and electrical conductivity of the Foxfonna proglacial river station in 2010, 2014, 2018 and 2019 are shown in Fig. 3. They demonstrate significant increases in bulk runoff EC during flow recessions, indicating the increasing dominance of the Proglacial Spring and (during 2018 and 2019) other downstream baseflow components during cold periods. The EC of the proglacial spring is far greater than that for bulk runoff and shows no evidence of diurnal variations like those observed in the bulk runoff EC records (caused by dilution from the Eastern Portal and other inputs from the glacier). The exception is the clear dilution associated with the peak discharge during the very short period of successful data collection in 2010. Otherwise, after 2010 the EC of the Proglacial spring increased and showed less seasonal dilution. For 2010 and 2014, the effects of the monitoring station's proximity to the glacier and the Proglacial Spring result in better-defined diurnal cycles at the Upper Bulk Station than during 2018 and 2019 at the Lower Bulk Station. Shallow groundwater and hyporheic zone inputs were observed while walking to the Lower Bulk Station and clearly increase the EC of bulk runoff compared to what was observed upstream during 2010 and 2014.

The results of the flow separation applied to the 2014 data showed an average outflow from the spring of the order of 30 ± 0.11 L/s. Fig. 4 indicates a relatively stable outflow, and no significant correlation with Qg, even after lagging the series to account for differences in the residence times of the various flow components.

4.2. Geochemistry of Foxfonna summer runoff

As was expected from the differences in EC shown in Fig. 3, major changes in the chemistry of bulk meltwater occurred after moving the sampling position from the Upper Bulk Station to the Lower Bulk Station. The principal differences between these two locations are significant SO_4^{2-}, Ca^{2+} and Mg^{2+} gains (Supplementary Table S1). Calculation of HCO_3^- by charge balance suggests only modest gains at the

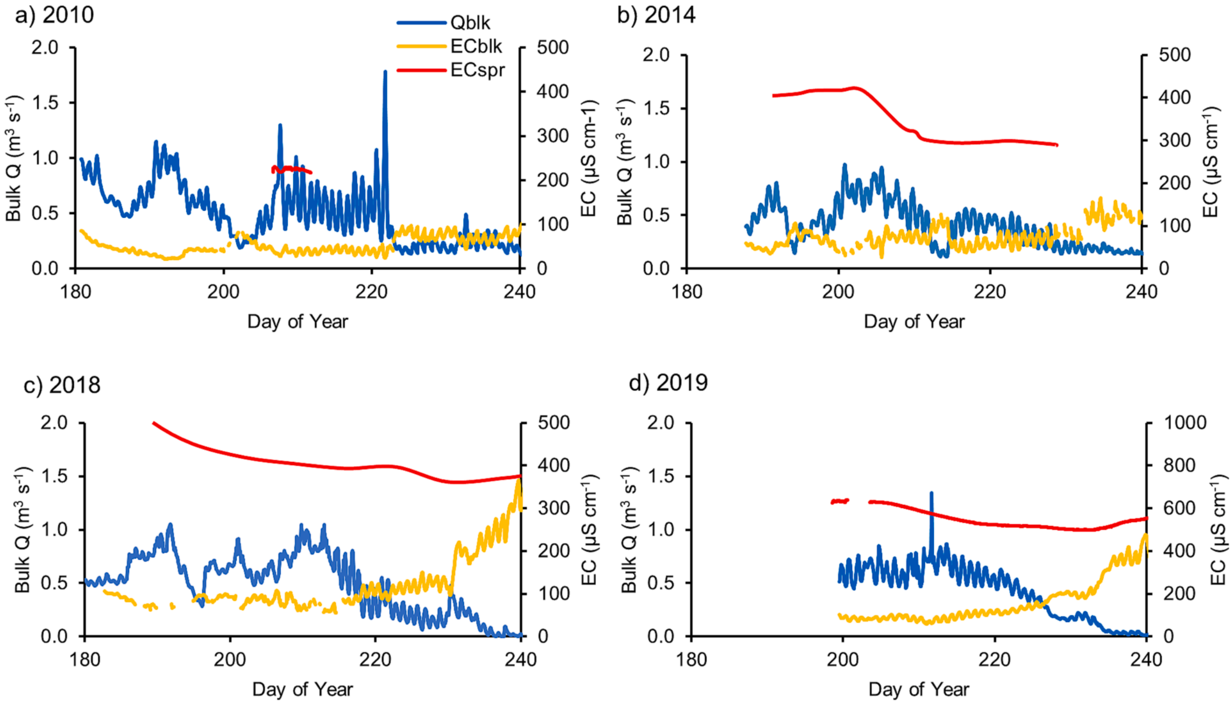

Fig. 3. Hydrological time series collected at the different sites shown in Fig. 2 through the study. "Qblk" and "ECblk" are the discharge and electrical conductivity in the bulk flow, whilst "ECspr" is the electrical conductivity in the Proglacial Spring.

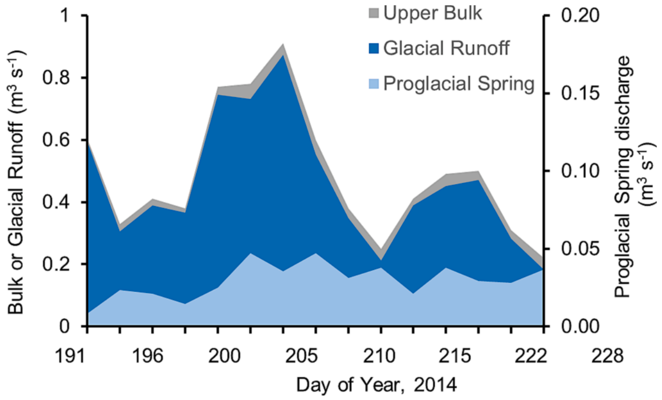

Fig. 4. Flow separation results quantifying seasonal changes in discharge at the Proglacial Spring and from the glacier, compared to the measured discharge at the Upstream Bulk station.

downstream station during early summer (2018) and even losses of HCO_3^- later on. Further upstream, the Proglacial Spring is notable for much higher Na^+ and HCO_3^- concentrations than anywhere else (Supplementary Table S1), and high Cl^- and SO_4^{2-} concentrations that were only matched by those recorded at the Lower Bulk Station during low flow (Fig. 5a and 5b). The Na^+/Cl^- ratios implied a non-marine source for most of the Na^+ observed at all sites (Fig. 5a). However, whilst the most dilute samples found at the glacier margin's Eastern Portal also demonstrated an excess of Na^+ relative to Cl^-, Ca^{2+} was by far the dominant cation here, with concentrations roughly double those of Na^+ and almost an order of magnitude greater than either Mg^{2+} or K^+ (Supplementary Table S1).

Apart from high Na^+ and HCO_3^- concentrations, the Proglacial Spring was notable for being anoxic and the only site where CH_4 was recorded. Here the ORP was typically (but not always) negative in 2018 and consistently negative in 2019. The lower ORP values were also associated with greater CH_4 concentrations (up to 2.1 mg L^{-1}), leading to a significant, negative correlation between the two parameters during the summer runoff period ($r = -0.82$, $p < 0.001$: Fig. 5c). A significant decline in the NO_3^- concentrations in the Proglacial Spring during recent years (Fig. 5d) means that NO_3^- concentrations became lower here than at either the East Portal, Upper Bulk or Lower Bulk sites. Proglacial Spring NO_3^- values in 2014 (average 0.21 ± 0.01 mg L^{-1}) were consistently high relative to those observed in subsequent years, and by 2019 they were all below the limit of detection (0.05 mg L^{-1}: Fig. 5d). Three opportunistic samples collected during 2022 suggest that NO_3^- concentrations have remained below detection limit.

Although the above variations in spring chemistry were largely inferred from just three summer sampling campaigns (2014, 2018 and 2019), the opportunistic measurements of EC in the summers of 2010, 2013, 2016 and 2017 can be used to supplement EC data from these years to indicate a longer-term trend of increasing solute concentrations in the Proglacial Spring (Fig. 5e and Supplementary Table S2). The most significant contributions to the increasing EC were the rising concentrations of SO_4^{2-} (Fig. 5f) and Na^+ (not shown).

4.3. *Geochemistry of winter samples*

Fig. 6a and Supplementary Table S3 show that the majority of proglacial springs during winter had EC values marginally in excess of those reported at Foxfonna during the summer, including Foxfonna itself (659 μS cm^{-1}). The generally higher EC of these springs was associated with higher ORP and $\delta^{13}C$-DIC (Fig. 6b and 6c), as well as more Ca^{2+} and Mg^{2+} (Supplementary Table S3). A bi-modal distribution of CH_4 concentrations was found, which were all in excess of saturation (about 0.08 μg/L) (Fig. 6d). Kleber et al (2023) show how super-saturation of CH_4 is typical of perennial proglacial springs in the Central Spitsbergen and is geogenic in origin (including at Foxfonna). The springs are also notable for markedly lower EC than the sub-permafrost groundwater springs in Adventdalen (range typically 3000 – 8000 μS cm^{-1}: Hodson et al., 2020). Lastly, there were no discernible differences between the composition of proglacial springs in the forefields of glaciers capable of supporting an expansive subglacial drainage system (due to the presence of temperate basal ice at Kokbreen, Drønbreen and Møysalbreen) and those unlikely to do so on account of the dominance of cold basal ice.

4.4. *Isotope geochemistry*

Fig. 6c shows that the $\delta^{13}C$-DIC typically lie in the range −12 to 0 ‰ VPDB, with by far the most observations lying towards the lower end of this range, especially in the Foxfonna Proglacial Spring during summer (Supplementary Tables S3 and S4). The $\delta^{34}S$-SO_4^{2-} values at Foxfonna in the summer were far higher (range 12 ‰ to 16 ‰ VCDT) than the winter spring samples (range −12 ‰ to 6.7 ‰ VCDT) (Supplementary Tables S3 and S4). The isotope composition of water for all samples (Fig. 7a) formed a regression relationship of $\delta D = 6.8\delta^{18}O - 9.1$ ($r^2 = 0.88$) and thus lay close to the Local Meteoric Water Line ($\delta D = 6.9\delta^{18}O - 0.3$) according to Retelle et al (2020). Foxfonna Proglacial Spring samples (Supplementary Table S4) lay well within the ranges observed in the winter spatial data set (-13 ‰ $< \delta O18 >$ -18 ‰ VSMOW and -130 ‰ $< \delta D >$ -95 ‰ VSMOW) (see Supplementary Table S3).

5. Discussion

Our multi-year summer observations from Foxfonna indicate a perennial, intra-permafrost groundwater flowpath at this site. Multi-site, winter observations also demonstrate that these groundwaters are discharging from almost all glacier forefields in the region. Such a widespread occurrence and obvious significance of perennial groundwater springs in glacier basins occupying the continuous permafrost zone of Central Spitsbergen was not expected, especially in cases where glaciers like Foxfonna have become cold-based and thus offer no obvious means of groundwater recharge via subglacial flowpaths. The following discussion therefore seeks to better understand the hydrology and biogeochemistry of these coupled glacier-groundwater systems by using Foxfonna as a case study. Thereafter we seek to establish the impact of ongoing glacier mass balance decline upon the biogeochemistry of the system through a temporal analysis of the Foxfonna data, before questioning its representativeness with an examination of the multi-site winter sampling.

5.1. *Hydrology of the Foxfonna proglacial groundwater spring*

Present-day estimates of Foxfonna's Proglacial Spring discharge are difficult to acquire on account of the highly unstable moraine that the artesian spring flows into. However, we have observed a drop in the pressure of the spring over the years to about half of that measured in 2014. According to the chemically-based mixing model, the average spring discharge in 2014 was 30 L S^{-1}, or 7.1 ± 4.1% of the total runoff at each time of sampling. The high Cl^- concentrations in the Foxfonna spring relative to bulk meltwaters at the glacier margin (Fig. 5a and Table S1: 2014 and 2018 data) indicate a greater proportion of snowmelt in the former (Tranter et al., 1996; Wadham et al., 1998). In fact, the concentrations of Cl^- show that there is little evidence of any glacial meltwater entering the Proglacial Spring, and so snow and/or firn in the upper catchment seem to dominate all the recharge meltwaters. Small bergschrund crevasses and rock fractures along the glacier's western margin between 1.3 and 2.0 km south of the spring represent the most plausible recharge pathway. Further south, the larger crevasses also allow firn and snow meltwaters to enter the glacier, but these waters enter the mine when they do so and are pumped out of the catchment. Visits to the mine showed that it is clearly isolated from the Proglacial Spring, which also pre-dates mining activity at the site by at least 14 years.

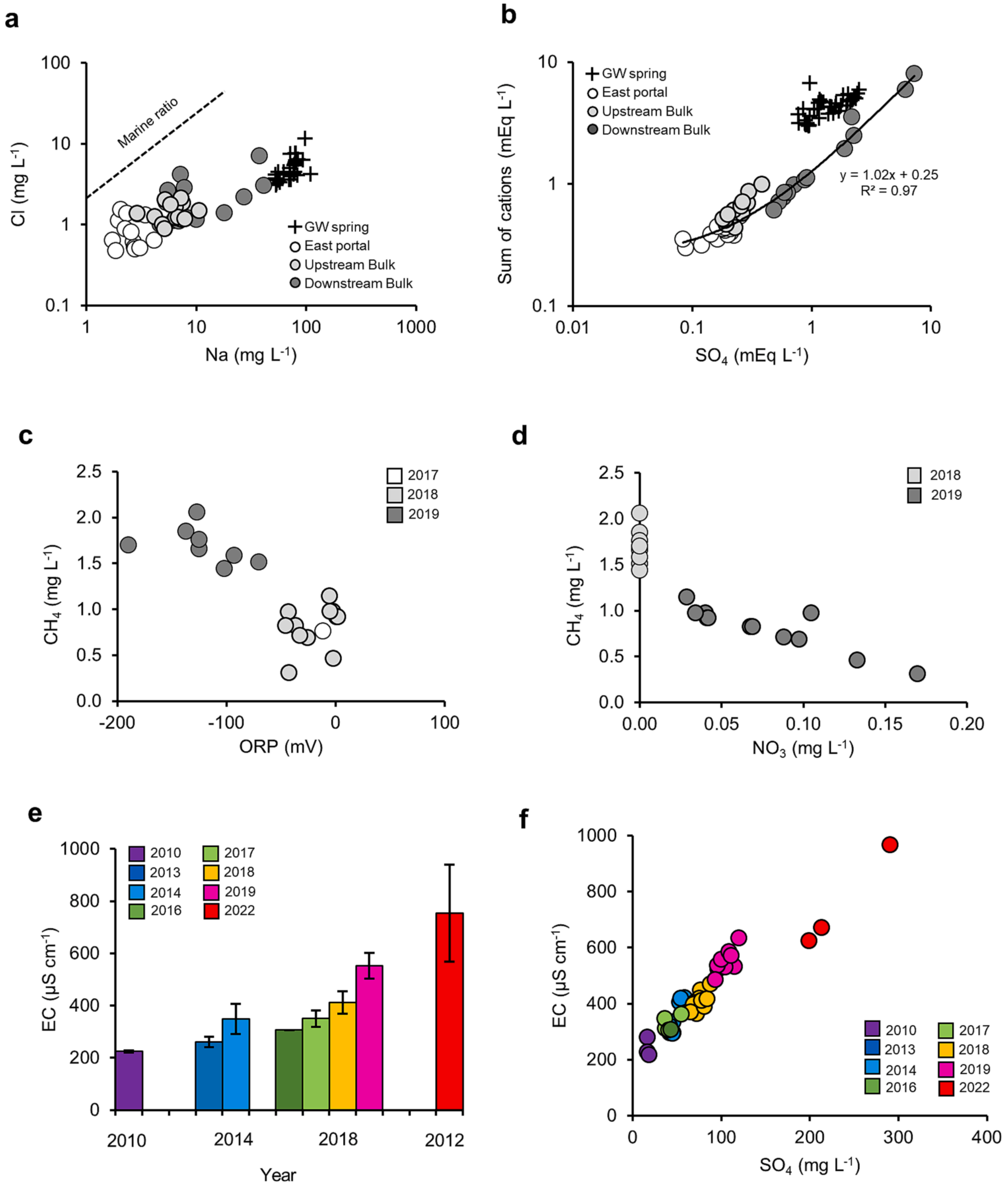

Fig. 5. Summer geochemistry at Foxfonna. a) and b): major ion characteristics at the different sites in Fig. 2; c) and d): CH_4 and NO_3^- relationships with ORP in the Foxfonna Proglacial Spring; e) and f): changing EC and its relationship with SO_4^{2-} in Foxfonna Proglacial Spring since 2010.

5.2. Solute acquisition at Foxfonna

Focussing upon 2014 provides useful insights into the different rock-water contact environments afforded by the various flowpaths closest to the glacier. The clearest difference is the cation composition, with Na^+-dominant Proglacial Spring waters clearly affecting the upstream bulk meltwaters after mixing with dilute glacial runoff from the Eastern portal (Fig. 5a). The 2018 and 2019 data from the Lower Bulk Station, however, show that significant gains in all cations are possible, most likely after acid hydrolysis reactions driven by sulphide oxidation. This is a well-known mechanism, described in many surface and near-surface flow paths that offer high rock-water contact in the area (Yde et al., 2008; Hindshaw et al., 2016; Jones et al., 2020; Hodson et al., 2016). When this is the dominant mechanism a strong relationship between SO_4^{2-} and cation concentrations results, provided waters remain under-saturated with respect to key mineral phases like calcite. When using equivalent units, the slope of the relationship between the sum of cations liberated and the SO_4^{2-} concentration is unity for silicate mineral dissolution, and two for the case of carbonate weathering (e.g. Hindshaw et al., 2016). For example, for every 8 mol (16 equivalents) of SO_4^{2-} produced by pyrite oxidation, albite weathering (Equation (3)) furnishes 16 equivalents of Na^+ cations, whilst calcite weathering (Equation (4)) furnishes 32 equivalents of Ca^{2+}:

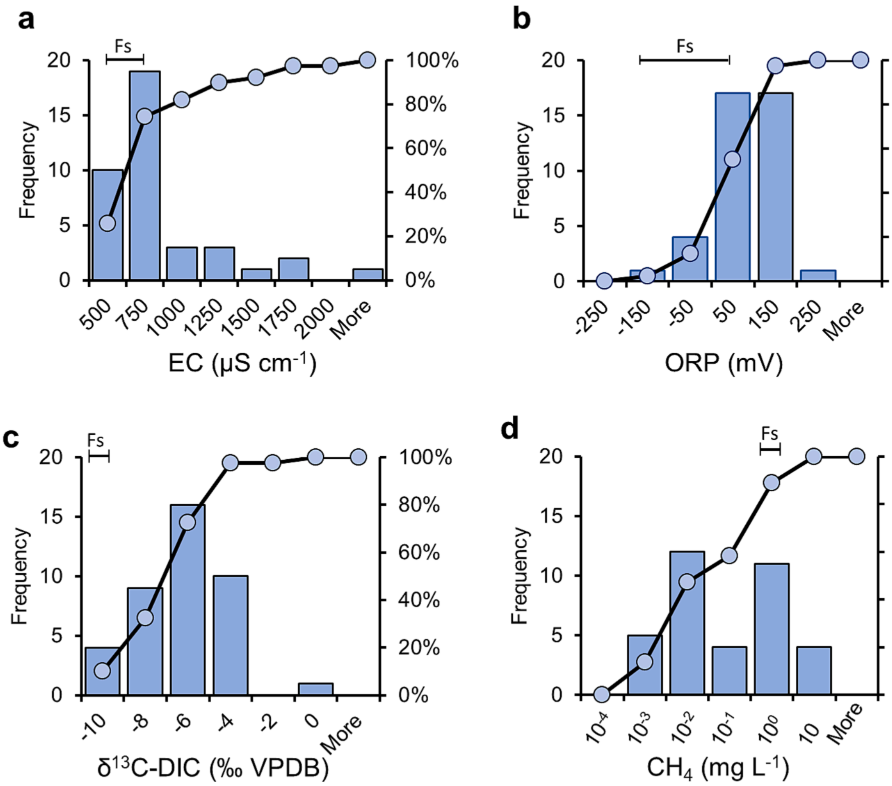

Fig. 6. Histograms showing the distribution of key geochemical parameters in the winter proglacial springs sampled at glaciers shown in Fig. 1. "Fs" denotes the bin (s) occupied by summer Foxfonna summer data. The solid line depicts the cumulative distribution.

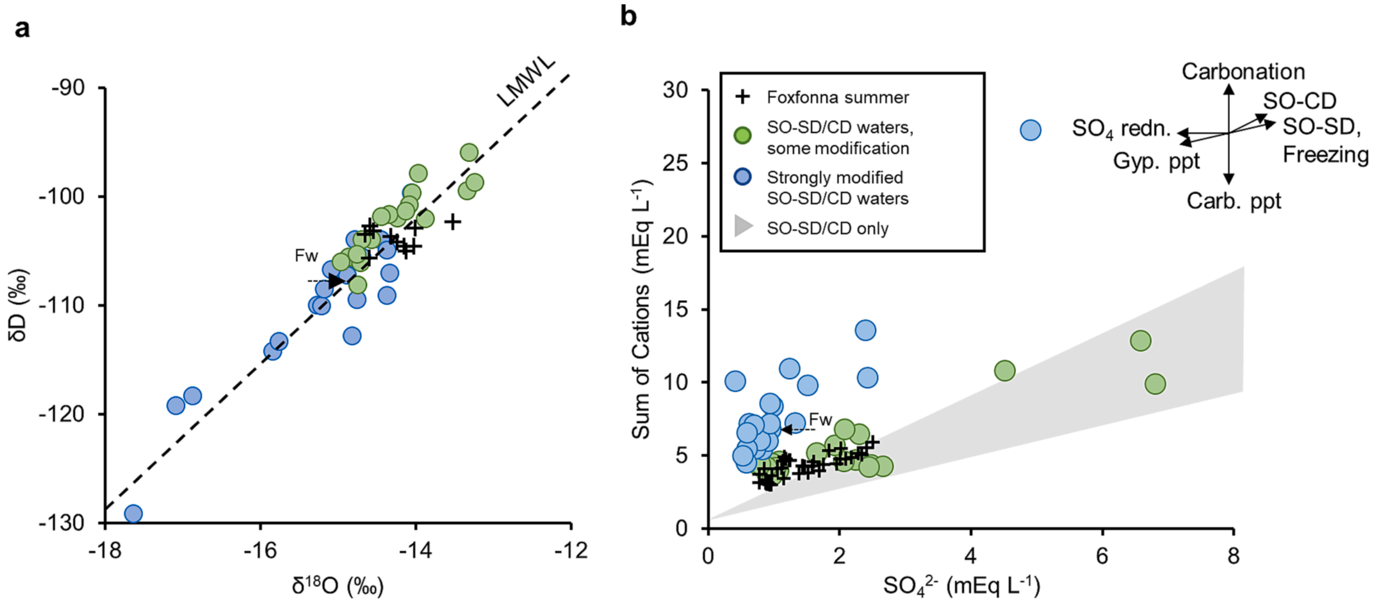

Fig. 7. Winter sampling results: a) water isotope composition: δ^{18}O-H_2O and δD-H_2O VSMOW, and b) major ion characteristics. "LMWL" is the Local Meteoric Water Line (after Retelle et al., 2020). Different coloured data points show two sample types distinguished according to their cation-SO_4^{2-} relationship, not different locations. The gray shaded area represents the domain produced solely by sulfide oxidation coupled to either silicate dissolution ("SO-SD") or carbonate dissolution ("SO-CD"). "Fw" shows the single winter sample collected from Foxfonna Proglacial Spring, whilst black crosses show all available summer data from the Proglacial Spring.

$$4FeS_{2(s)} + 16NaAlSi_3O_{8(s)} + 15O_{2(aq)} + 86H_2O_{(l)} \leftrightarrow 4Fe(OH)_{3(s)} + 16Na^+_{(aq)} + 4Al_4Si_4O_{10}(OH)_{8(s)} + 32H_4SiO_{4(aq)} + 8SO^{2-}_{4(aq)} \quad (4)$$

Or,

$$4FeS_{2(s)} + 16CaCO_{3(s)} + 15O_{2(aq)} + 14H_2O_{(l)} \leftrightarrow 4Fe(OH)_{3(s)} + 16Ca^{2+}_{(aq)} + 16HCO^-_{3(aq)} + 8SO^{2-}_{4(aq)} \quad (5)$$

Fig. 5b shows a particularly strong relationship with a slope very close to unity (i.e. 1.02) between SO_4^{2-} and total cations in the Eastern Portal (2014) and the Downstream Bulk (2018) sites. The intercept is just 0.25, and presumably identifies an additional contribution of cations from other sources (snowmelt, carbonation reactions, etc: see Hodson and Yde, 2022). Therefore the dominant weathering mechanism in these well aerated waters gaining rock-water contact along the glacier margin and in the glacier forefield seems to be the coupling of sulphide oxidation to silicate mineral dissolution, rather than carbonate dissolution. An almost identical relationship (slope 1.0, intercept 0.21) was also found by Hindshaw et al (2016) in non-glacierised headwaters draining near-identical rock formations to the present study. These artefacts are fairly unusual in the Svalbard literature, except where carbonate-poor sandstones and shales are encountered. At Foxfonna, it is the Firkanten Formation which hosts the groundwater flowpath: a formation that is known for its high pyrite content and virtually no carbonate (Dixon, 2019).

By contrast to the Eastern Portal and Lower Bulk samples, the high SO_4^{2-} concentrations in the Proglacial Spring are acquired from the same rock formations, yet have a weaker association with the sum of cations and plot in a different domain of the graph. Their position relative to the regression model in Fig. 5b suggests SO_4^{2-} removal (displacement from right to left), although it is not inconceivable that it was caused by other weathering reactions such as carbonation (displacement vertically), if a source of CO_2 is available (see below). Mineral precipitation (e.g. gypsum or calcite) cannot explain the domain of the graph occupied by the Proglacial Spring samples either (since both cations and SO_4^{2-} are removed from solution). Removal of SO_4^{2-} by microbial sulfate reduction (Equation (5)) yields bicarbonate derived from organic matter (e.g. Jones et al., 2020; Wadham et al., 2004). This process would explain both the lower than expected SO_4^{2-} and the low δ^{13}C-DIC values found in the proglacial spring (Supplementary Table S4). Wadham et al (2004) demonstrated the clear impact of SO_4^{2-} reduction upon δ^{13}C-DIC at another Svalbard glacier, Finsterwalderbreen, but here the presence of calcite meant that δ^{13}C-DIC values were greater than those in the present study. This work also demonstrated the well-known fractionation effect upon the residual SO_4^{2-} in long residence time, anoxic subglacial waters, causing an increase in δ^{34}S-SO_4^{2-}. Values for the Foxfonna Proglacial Spring in 2019 (12‰ to 16 ‰ VCDT: Supplementary Table S4) clearly show this is the case, since they far exceed the range of δ^{34}S values identified in the local bedrock by Dixon (2019) (range: −40.06 ‰ to −2.04 ‰ VCDT). Pyrite δ^{34}S of −5.4 ‰ and −7.4 ‰ VCDT were also found by Hindshaw et al (2016) in Fardalen headwaters about 13 km to the west of the Proglacial Spring.

$$2CH_2CO + SO^{2-}_{4(aq)} \leftrightarrow 2HCO^-_{3(aq)} + H_2S_{(g)} \quad (6)$$

Given the above, all flowpaths in the system attest to the importance of sulfide oxidation leading to cation acquisition via silicate mineral weathering, although this is far less important in the dilute waters of the Eastern Portal. However, the presence of anoxic conditions, detectable CH_4 and clear evidence for sulfate reduction show that the composition of waters discharging from the Proglacial Spring is further modified to a significant degree by processes indicative of more strongly reducing conditions.

5.3. *Changing biogeochemistry of the Foxfonna Proglacial Spring*

Several important changes in the chemistry of the Proglacial Spring were described above, including significant increases in EC and the concentrations of SO_4^{2-} and Na^+, and a complete loss of NO_3^- (Fig. 5d – 5f and Supplementary Tables S1 and S3). There is also evidence for decreasing ORP and increasing CH_4 concentrations, although comprehensive data are only available for the summer runoff seasons in 2018 and 2019 (Fig. 5c). Collectively, these changes imply the system is receiving lower recharge volumes of dilute meltwaters derived from the surface environment. The reduced recharge is likely to have been exacerbated by the formation of permafrost at the glacier bed (e.g. Haldorsen et al., 2010) and a marked reduction in the firn area along the flanks of the glacier, where recharge waters for the groundwater are sourced (Fig. 2). As a consequence, artesian pressures at the outflow have dropped and residence time within the groundwater system is likely to have increased, resulting in a more concentrated, anoxic outflow than initially observed in 2010. The result is an increase in the impact of sulfide oxidation, driving the concentrations of SO_4^{2-} and Na^+ upwards and maintaining a high oxygen demand. For these reasons, SO_4^{2-} concentrations showed the strongest correlation with the ORP during the detailed sampling campaigns of summer 2018 and 2019 ($r = 0.86$, $p < 0.001$). However, the correlation was not significant when the low SO_4^{2-} concentrations prior to 2018 season were included (suggesting sulfide oxidation was less influential upon ORP when flows were higher).

Another noticeable change in the composition of the Proglacial Spring during the observation period was the loss of NO_3^-. Two potential processes require consideration in this context: first, a reduction in the efficacy of NO_3^- supply by nitrification; and second, an increase in the impact of denitrification (e.g. Wynn et al., 2006). Both explanations become increasingly plausible as the system is driven towards more reducing conditions by sulphide oxidation, making their relative importance difficult to establish. Several studies have reported the generation of so-called “excess NO_3^-” in Svalbard glacial meltwaters by nitrification in oxic, high rock-water contact environments (Ansari et al., 2013; Hodson et al., 2005; Wynn et al., 2007). This results in high NO_3^-/Cl^- ratios relative to the snowpack or snowmelt, which are dominated by atmospheric inputs. For example NO_3^-/Cl^- ratios at the Eastern Portal samples (average 0.25 ± 0.19 in mg L^{-1} units using data in Supplementary Table S1) often exceed those of typical Svalbard snow cover (<0.09: Wynn et al., 2007) and thus reveal the likely influence of nitrification. Far higher NO_3^-/Cl^- ratios were also apparent in the Lower Bulk Station samples of 2018 (average 0.62 ± 0.44). However, high NO_3^-/Cl^- ratios were never observed in Proglacial Spring samples (e.g. 0.05 ± 0.2 in 2014, 0.02 ± 0.01 in 2018 and zero thereafter). These values mean that there is no evidence for an additional input of NO_3^- from nitrification in the groundwater flowpath at any time. However, the consistently lower NO_3^-/Cl^- ratios in the Proglacial Spring compared to other active flowpaths, reveal that denitrification has been occurring throughout the study (or at least from 2014 onwards). Denitrification has also become more influential during the recent changes in the redox conditions of the ground water flowpath, resulting in values consistently below detection limits.

5.4. *Geochemistry of winter Proglacial springs*

Fig. 7b shows that SO_4^{2-} concentrations in the different proglacial spring samples were all in excess of 0.42 mEq L^{-1}, demonstrating appreciable sulfide oxidation at all sites (in the absence of other SO_4^{2-} sources in the area). The relationship between SO_4^{2-} and the sum of cations is also shown, and two distinct groups are apparent that overlap at low concentrations: 1) a low cation concentration group which lies in a domain of the graph also occupied by summer samples from the Proglacial Spring at Foxfonna, and presumably shares a similar origin; and 2) a high concentration group that includes the only available winter sample from Foxfonna. It is difficult to attribute cation acquisition by the second group to acid hydrolysis following sulfide oxidation alone (i.e. Equations (3) and (4)), because the slope of the relationship shown in Fig. 5b (in equivalent units) is in excess of 4. The vector diagram in Fig. 7b shows that several additional processes could be responsible for this problem. First, they could be displaced towards the origin of the X axis if they subsequently experienced more SO_4^{2-} reduction than the other group (after acquiring SO_4^{2-} by sulfide oxidation). However, in most cases they display higher δ^{13}C-DIC signatures than is the case at Foxfonna during summer (Fig. 5c), indicating the presence of atmospheric or carbonate-derived DIC, rather than a depleted δ^{13}C-DIC signature as observed in the Foxfonna Proglacial Spring during summer. Second, these samples might be derived from flowpaths where sulphide oxidation is less important than carbonation reactions (i.e. the vertical vector in Fig. 7b). Since the surplus of cations relative to SO_4^{2-} is dominated by Na^+, then albite carbonation could be the most important mechanism (Equation (7)):

$$2NaAlSi_3O_{8(s)} + 2CO_{2(aq)} + 11H_2O_{(l)} \leftrightarrow 2Na^+_{(aq)} + Al_2Si_2O_5(OH)_{4(s)} + 4H_4SiO_{4(aq)} + 2HCO^-_{3(aq)} \quad (7)$$

Further examination of this group of springs also showed that samples with the lowest $\delta^{18}O$-H_2O and δD-H_2O (see Fig. 7a) also had the highest solute concentrations. Partial freezing could explain these artefacts, due to the rejection of solute and dissolved gases from the ice phase (Killawee et al., 1998), which at the same time preferentially incorporates heavier water isotopes (i.e. ^{18}O and Deuterium: Lacelle, 2011). In some cases, O_2 super-saturation (>14.10 mg L^{-1} in Supplementary Table S3) was also observed, suggesting that some oxygen is likely to have been acquired prior to freeze-concentration. In these cases, freezing is likely to have occurred following discharge into the glacier floodplain and during temporary storage beneath the proglacial icing (e.g. an air pocket within an icing blister: see Kleber et al., 2023)). Such conditions are not at all representative of a pressurised groundwater flowpath, and so these data are of limited utility. However, two samples from Kokbreen's immediate ice margin showed the lowest $\delta^{18}O$-H_2O and δD-H_2O values in the entire data set, but no signs of oxidation (Supplementary Table S3). We tentatively suggest that this is the only site demonstrating freezing effects that were influential along the groundwater flowpath, potentially revealing a spring that will ultimately cease to flow.

6. Conclusions

Perennial springs are extremely common in the forefields of Svalbard glaciers and appear to discharge groundwaters with a composition commensurate with the extended residence times necessary to maintain flow through the long, cold winter season. Observations of ground temperatures around and beneath the cold-based Foxfonna show that this can be achieved via intra-permafrost ground water flow, not sub-permafrost flow. The geochemistry of springs in neighbouring glaciers suggest the same is the case elsewhere, and so subglacial drainage networks are not necessary for groundwater recharge. This is contrary to expectation, because the existing paradigm proposed that, as glaciers lose mass in response to more intense ablation during summer, their transition to cold-based thermal regime should effectively seal off aquifers from subglacial recharge. Evidence for partial freezing during transit through the groundwater flowpaths was present, but by no means common. In fact our study shows that sufficient recharge via bergschrund crevasses and bedrock fractures can maintain active ground water flow, at least for some years. However, we do find evidence that these intra-permafrost groundwaters are transient, and perhaps represent a legacy inherited from when the glaciers supporting them were polythermal. At Foxfonna, the groundwater outflow is becoming less vigorous and more concentrated as time passes, most likely because the firn area that recharges the groundwater (via bergschrund crevasses) is in significant decline due to net ablation. Biogeochemical processes, especially sulfide oxidation and denitrification, exert an increasing influence upon outflow chemistry as flow rates decline. Glacier-groundwater coupling in the permafrost zone of the high Arctic is clearly more important than hitherto appreciated, and so its role in biogeochemical processes at the landscape scale deserves more attention.

CRediT authorship contribution statement

Andrew Hodson: Conceptualization, Funding acquisition, Investigation, Data curation, Writing – original draft, Editing. **Gabrielle Kleber:** Investigation, Writing – review & editing. **Jack Johnson:** Investigation, Writing – review & editing. **Michael Lonardi:** Investigation, Writing – review & editing. **Chiara Petroselli:** Investigation, Writing – review & editing. **Tim Dixon:** Investigation, Writing – review & editing. **Simon Bottrell:** Writing – review & editing.

Declaration of Competing Interest

The authors declare the following financial interests/personal relationships which may be considered as potential competing interests: Andrew Hodson reports financial support was provided by Research Council of Norway. Andrew Hodson reports financial support was provided by Royal Geographical Society. Andrew Hodson reports financial support was provided by Joint Programming Initiative Climate.

Data availability

Data will be made available on request.

Acknowledgements

This work was funded by a Joint Programming Initiative (JPI-Climate Topic 2: Russian Arctic and Boreal Systems) Award No. 71126, UK Natural Environment Research Council grant NE/M019829/1, Research Council of Norway grant (NRC no. 294764) and a Royal Geographical Society Ralph Brown Expedition Award 2017.

Appendix A. Supplementary data

Supplementary data to this article can be found online at https://doi.org/10.1016/j.jhydrol.2023.129894.

References

Ansari, A.H., Hodson, A.J., Heaton, T.H.E., Kaiser, J., Marca-Bell, A., 2013. Stable isotopic evidence for nitrification and denitrification in a High Arctic glacial ecosystem. Biogeochemistry 113 (1-3), 341–357.

Chesnokova, A., Baraër, M., Bouchard, É., 2020. Proglacial icings as records of winter hydrological processes. Cryosphere 14, 4145–4164.

Christiansen, H.H., French, H.M., Humlum, O., 2005. Permafrost in the Gruve-7 mine, Adventdalen, Svalbard. Norsk Geografisk Tidsskrift-Norwegian J. Geogr. 59 (2), 109–115.

Cooper, R.J., Wadham, J.L., Tranter, M., Hodgkins, R., Peters, N.E., 2002. Groundwater hydrochemistry in the active layer of the proglacial zone, Finsterwalderbreen, Svalbard. J. Hydrol. 269 (3–4), 208–223.

Dixon, T.J., 2019. Geogenic Nitrogen as a Nutrient Source to Subglacial Microbial Ecosystems (Doctoral dissertation). University of Leeds.

Etzelmüller, B., Hagen, J.O., 2005. Glacier-permafrost interaction in Arctic and alpine mountain environments with examples from southern Norway and Svalbard. Geol. Soc. Lond. Spec. Publ. 242 (1), 11–27.

Haldorsen, S., Heim, M., Dale, B., Landvik, J.Y., van der Ploeg, M., Leijnse, A., Salvigsen, O., Hagen, J.O., Banks, D., 2010. Sensitivity to long-term climate change of subpermafrost groundwater systems in Svalbard. Quat. Res. 73 (2), 393–402.

Hindshaw, R.S., Heaton, T.H., Boyd, E.S., Lindsay, M.R., Tipper, E.T., 2016. Influence of glaciation on mechanisms of mineral weathering in two high Arctic catchments. Chem. Geol. 420, 37–50.

Hodgkins, R., Hagen, J.O., Hamran, S.E., 1999. 20th century mass balance and thermal regime change at Scott Turnerbreen, Svalbard. Ann. Glaciol. 28, 216–220.

Hodson, A.J., Ferguson, R.I., 1999. Fluvial suspended sediment transport from cold and warm-based glaciers in Svalbard. Earth Surf. Proc. Land. 24 (11), 957–974.

Hodson, A.J., Mumford, P.N., Kohler, J., Wynn, P.M., 2005. The High Arctic glacial ecosystem: new insights from nutrient budgets. Biogeochemistry 72 (2), 233–256.

Hodson, A., Nowak, A., Christiansen, H., 2016. Glacial and periglacial floodplain sediments regulate hydrologic transfer of reactive iron to a high arctic fjord. Hydrol. Process. 30 (8), 1219–1229.

Hodson, A.J., Nowak, A., Hornum, M.T., Senger, K., Redeker, K., Christiansen, H.H., Jessen, S., Betlem, P., Thornton, S.F., Turchyn, A.V., Olaussen, S., 2020. Sub-permafrost methane seepage from open-system pingos in Svalbard. Cryosphere 14 (11), 3829–3842.

Hodson, A.J. and Yde, J.C. 2022. The geochemistry of glacial meltwaters. In Shroder, J.F. (ed.): Treatise on geomorphology, second edition, volume 4. Elsevier, Academic Press, 290-304. https://doi.org/10.1016/B978-0-12-818234-5.00145-0.

Humlum, O., Instanes, A., Sollid, J.L., 2003. Permafrost in Svalbard: a review of research history, climatic background and engineering challenges. Polar Res. 22 (2), 191–215.

Irvine-Fynn, T.D.L., Hodson, A.J., 2010. Biogeochemistry and dissolved oxygen dynamics at a subglacial upwelling, Midtre Lovénbreen, Svalbard. Ann. Glaciol. 51 (56), 41–46.

Isaksen, K., Sollid, J.L., Holmlund, P., Harris, C., 2007. Recent warming of mountain permafrost in Svalbard and Scandinavia. J. Geophys. Res. 112, F02S04.

Jones, E.L., Hodson, A.J., Thornton, S.F., Redeker, K.R., Rogers, J., Wynn, P.M., Dixon, T. J., Bottrell, S.H., O'Neill, H.B., 2020. Biogeochemical processes in the active layer and permafrost of a high Arctic fjord valley. Front. Earth Sci. 8, 342.

Killawee, J.A., Fairchild, I.J., Tison, J.-L., Janssens, L., Lorrain, R., 1998. Segregation of solutes and gases in experimental freezing of dilute solutions: Implications for natural glacial systems. Geochim. Cosmochim. Acta 62 (23-24), 3637–3655.

Kleber, G.E., Hodson, A., Turchyn, A.V., Magerl, L., Mannerfelt, E.S., Bradbury, H.J., 2023. Glacial retreat driving enhanced methane emissions in the high Arctic. Nature Geosciences. https://doi.org/10.1038/s41561-023-01210-6.

Kristiansen, S.M., Yde, J.C., Bárcena, T.G., Jakobsen, B.H., Olsen, J., Knudsen, N.T., 2013. Geochemistry of groundwater in front of a warm-based glacier in southeast greenland. Geogr. Ann. Ser. B 95 (2), 97–108.

Lacelle, D., 2011. On the δ^{18}O, δD and D-excess relations in meteoric precipitation and during equilibrium freezing: theoretical approach and field examples. Permafr. Periglac. Process. 22 (1), 13–25.

Lauritzen, S.E., Bottrell, S., 1994. Microbiological activity in thermoglacial karst springs, south Spitzbergen. Geomicrobiol J. 12, 161–173.

Liestøl, O. 1974. Glaciological work in 1972. Norsk Polarinstitutt Arbok 1974, 125–135.

Nowak, A., Hodson, A., 2014. Changes in meltwater chemistry over a 20-year period following a thermal regime switch from polythermal to cold-based glaciation at Austre Broggerbreen, Svalbard. Polar Res. 33 (1), 22779.

Ó Dochartaigh , B.É. , MacDonald , A.M. , Black , A.R. , Everest , J. , Wilson , P. , Darling , W.G. , Jones , L. , Raines , M. , 2019 . Groundwater–glacier meltwater interaction in proglacial aquifers . Hydrol. Earth Syst. Sci. 23 (11), 4527 – 4539.

Orvin, A.K., 1944. Litt om kilder på Svalbard. (A note on the springs of Svalbard.) Nor. Geogr. Tidsskr. 10, 1–26.

Nowak, A.; Hodgkins, R.; Nikulina, A.; Osuch, M.; Wawrzyniak, T.; Kavan, J.; Łepkowska, E.; Majerska, M.; Romashova, K.; Vasilevich, I. 2020. From land to fjords: The review of Svalbard hydrology from 1970 to 2019 (SvalHydro). SESS Report 2020-The State of Environmental Science in Svalbard-An Annual Report, Svalbard Integrated Arctic Earth Observing System, 2021; 176–201.

Retelle, M., Christiansen, H.H., Hodson, A., Nikulina, A., Osuch, M., Poleshuk, K.R., Roof, S., Rouyet, L., Strand, S.M., Vasilevich, I. and Wawrzyniak, T. 2020. Environmental Monitoring in the Kapp Linné-Grønfjorden Region (KLEO) in Van den Heuvel et al. (eds.): SESS report 2019, Svalbard Integrated Arctic Earth Observing System, Longyearbyen. *SESS report.*

Scheidegger, J.M., Bense, V.F., 2014. Impacts of glacially recharged groundwater flow systems on talik evolution. J. Geophys. Res. Earth 119 (4), 758–778.

Schuler, T.V., Kohler, J., Elagina, N., Hagen, J.O.M., Hodson, A.J., Jania, J.A., Kääb, A. M., Luks, B., Małecki, J., Moholdt, G., Pohjola, V.A., Sobota, I., Van Pelt, W.J.J., 2020. Reconciling Svalbard glacier mass balance. Front. Earth Sci. 8.

Schytt Holmlund, E., 2020. Rapid Temperature Rise may have Triggered Glacier Surges all Over Svalbard. UiT Norges Arktiske Universitet. Master's thesis.

Sevestre, H., Benn, D.I., Hulton, N.R., Bælum, K., 2015. Thermal structure of Svalbard glaciers and implications for thermal switch models of glacier surging. J. Geophys. Res. Earth 120 (10), 2220–2236.

Sharp, M., Brown, G.H., Tranter, M., Willis, I.C., Hubbard, B., 1995. Comments on the use of chemically based mixing models in glacier hydrology. J. Glaciol. 41 (138), 241–246.

Skidmore, M.L., Sharp, M.J., 1999. Drainage system behaviour of a High-Arctic polythermal glacier. Ann. Glaciol. 28, 209–215.

Smith, A.M., Murray, T., Davison, B.M., Clough, A.F., Woodward, J., Jiskoot, H., 2002. Late surge glacial conditions on Bakaninbreen, Svalbard, and implications for surge termination. J. Geophys. Res.: Solid Earth 107 (B8), ESE-1.

Stachniak, K., Sitek, S., Ignatiuk, D., Jania, J., 2022. Hydrogeological model of the forefield drainage system of Werenskioldbreen. Svalbard. Water 14 (9), 1514.

Stachnik, Ł., Yde, J.C., Kondracka, M., Ignatiuk, D., Grzesik, M., 2016. Glacier naled evolution and relation to the subglacial drainage system based on water chemistry and GPR surveys (Werenskioldbreen, SW Svalbard). Ann. Glaciol. 57 (72), 19–30.

Szynkiewicz, A., Olichwer, T., Tarka, R., 2020. Delineation of groundwater provenance in Arctic environment using isotopic compositions of water and sulphate. J. Hydrol. 580, 124232.

Tranter, M., Brown, G.H., Hodson, A.J., Gurnell, A.M., 1996. Hydrochemistry as an indicator of subglacial drainage system structure: A comparison of alpine and sub-polar environments. Hydrol. Process. 10 (4), 541–556.

Van Pelt, W.J., Pohjola, V.A., Reijmer, C.H., 2016. The changing impact of snow conditions and refreezing on the mass balance of an idealized Svalbard glacier. Front. Earth Sci. 4, 102.

Vincent, A., Violette, S., Aðalgeirsdóttir, G., 2019. Groundwater in catchments headed by temperate glaciers: A review. Earth Sci. Rev. 188, 59–76.

Wadham, J.L., Hodson, A.J., Tranter, M., Dowdeswell, J.A., 1998. The hydrochemistry of meltwaters draining a polythermal-based, high Arctic glacier, south Svalbard: I. The ablation season. Hydrol. Processes 12 (12), 1825–1849.

Wadham, J.L., Bottrell, S., Tranter, M., Raiswell, R., 2004. Stable isotope evidence for microbial sulphate reduction at the bed of a polythermal high Arctic glacier. Earth Planet. Sci. Lett. 219 (3–4), 341–355.

Wadham, J.L., Tranter, M., Skidmore, M., Hodson, A.J., Priscu, J., Lyons, W.B., Sharp, M., Wynn, P., Jackson, M., 2010. Biogeochemical weathering under ice: size matters. Global Biogeochem. Cycles 24 (3).

Wainstein, P., Moorman, B., Whitehead, K., 2014. Glacial conditions that contribute to the regeneration of Fountain Glacier proglacial icing, Bylot Island, Canada. Hydrol. Processes 28 (5), 2749–2760.

Wynn, P.M., Hodson, A., Heaton, T., 2006. Chemical and isotopic switching within the subglacial environment of a High Arctic glacier. Biogeochemistry 78 (2), 173–193.

Wynn, P.M., Hodson, A.J., Heaton, T.H., Chenery, S.R., 2007. Nitrate production beneath a High Arctic glacier, Svalbard. Chem. Geol. 244 (1–2), 88–102.

Yde, J.C., Riger-Kusk, M., Christiansen, H.H., Knudsen, N.T., Humlum, O., 2008. Hydrochemical characteristics of bulk meltwater from an entire ablation season, Longyearbreen, Svalbard. J. Glaciol. 54 (185), 259–272.